Synergy of atom-probe structural data and quantum-mechanical calculations in a theory-guided design of extreme-stiffness superlattices containing metastable phases

2015 New J. Phys. 17 093004

(http://iopscience.iop.org/1367-2630/17/9/093004)

New Journal of Physics
The open access journal at the forefront of physics

Deutsche Physikalische Gesellschaft DPG
IOP Institute of Physics

Published in partnership with: Deutsche Physikalische Gesellschaft and the Institute of Physics

OPEN ACCESS

RECEIVED
10 April 2015

REVISED
16 July 2015

ACCEPTED FOR PUBLICATION
30 July 2015

PUBLISHED
2 September 2015

PAPER

Synergy of atom-probe structural data and quantum-mechanical calculations in a theory-guided design of extreme-stiffness superlattices containing metastable phases

M Friák[1,2], D Tytko[1], D Holec[3], P-P Choi[1], P Eisenlohr[1,4], D Raabe[1] and J Neugebauer[1]

[1] Max-Planck-Institut für Eisenforschung GmbH, D-40237 Düsseldorf, Germany
[2] Institute of Physics of Materials, Academy of Sciences of the Czech Republic, v. v. i., 61662 Brno, Czech Republic
[3] Montanuniversität Leoben, A-8700 Leoben, Austria
[4] Michigan State University, East Lansing, MI 48824, USA

E-mail: friak@ipm.cz

Keywords: superlattices, elasticity, *ab initio*, nitrides, Young's modulus, composites

Abstract

A theory-guided materials design of nano-scaled superlattices containing metastable phases is critically important for future development of advanced lamellar composites with application-dictated stiffness and hardness. Our study combining theoretical and experimental methods exemplifies the strength of this approach for the case of the elastic properties of AlN/CrN superlattices that were deposited by reactive radio-frequency magnetron sputtering with a bilayer period of 4 nm. Importantly, CrN stabilizes AlN in a metastable B1 (rock salt) cubic phase only in the form of a layer that is very thin, up to a few nanometers. Due to the fact that B1-AlN crystals do not exist as bulk materials, experimental data for this phase are not available. Therefore, quantum-mechanical calculations have been applied to simulate an AlN/CrN superlattice with a similar bilayer period. The *ab initio* predicted Young's modulus (428 GPa) along the [001] direction is in excellent agreement with measured nano-indentation values (408 $\pm$ 32 GPa). Aiming at a future rapid high-throughput materials design of superlattices, we have also tested predictions obtained within linear-elasticity continuum modeling using elastic properties of B1-CrN and B1-AlN phases as input. Using single-crystal elastic constants from *ab initio* calculations for both phases, we demonstrate the reliability of this approach to design nano-patterned coherent superlattices with unprecedented and potentially superior properties.

Introduction

Over the past decades, transition metal nitrides have found wide-spread technological application as protective coatings for improving the hardness, wear, oxidation and corrosion resistance of cutting tools and machine parts [1–16]. Initial research focused on monophase binary nitrides (TiN, CrN, NbN, VN, etc) [1–3]. Significantly improved performance was subsequently obtained by development of ternary, quaternary, and multinary single phase coatings, a typical prototype of which is e.g. $Ti_{1-x}Al_xN$ or $Cr_{1-x}Al_xN$ [17–19]. However, there is a constant need for novel advanced systems with yet more superior properties.

Compositionally modulated multilayers, and in particular superlattices with commensurate crystal structures and bi-layer periods in the range of a few nanometers, have proven to be a prospective concept for improving mechanical properties of nitride hard coatings [4–14, 20, 21]. Maximum hardness values from 35 to 50 GPa could be achieved by several types of superlattices (e.g. TiN/AlN [5], TiN/NbN [6], TiN/VN [7], TiN/CrN [8, 9, 20], AlN/CrN [10–12, 21]). Such a high hardness is comparable with cubic-BN and exceeded by only a few materials, such as diamond. In comparison to these materials, however, metal nitrides have the advantage of providing also high corrosion and oxidation resistance in addition to their excellent mechanical properties [4, 13–16]. In particular, AlN/CrN has been shown to possess an outstanding combination of all these properties [10–16, 21].

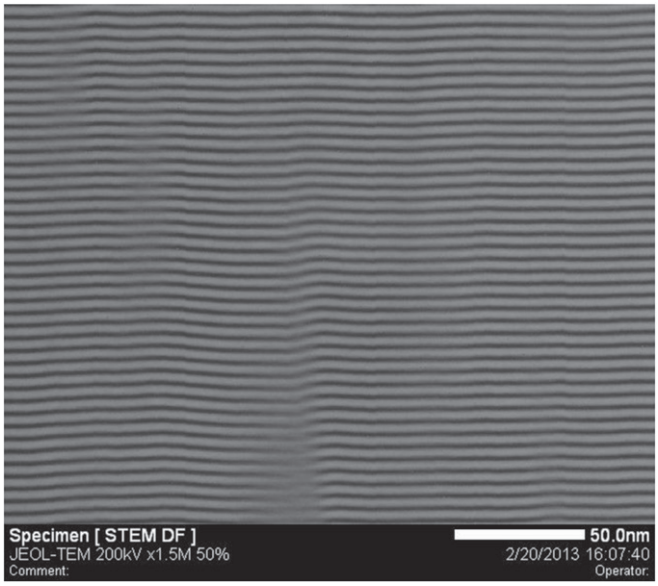

Figure 1. Scanning transmission electron microscopy (STEM) image of studied AlN/CrN coherent superlattice.

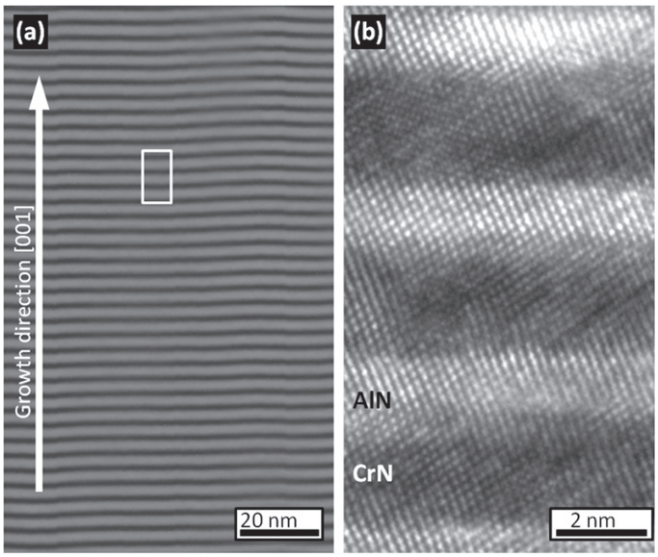

Figure 2. (a) Scanning transmission electron microscopy high angle annular dark field (STEM HAADF) image of the as-deposited AlN/CrN superlattice showing chemically sharp layers (bright and dark contrast corresponds to CrN and AlN, respectively); (b) high-resolution transmission electron microscopy (HR-TEM) image of the region marked by the rectangle in (a) showing coherent multilayers. The multilayers are stacked along the [001] direction.

We focus our study on AlN/CrN superlattices (see figures 1 and 2) that exhibit a hardness of up to 40 GPa [10–12, 21]. When only a few nm thin, the AlN (that crystallizes under ambient conditions in a hexagonal crystal phase) is stabilized in the cubic B1 (NaCl) structure [22]. Also, the Young's modulus of AlN/CrN superlattices is very high: nano-indentation reveals a range of 408 $\pm$ 32 GPa in case of the as-deposited samples in the direction perpendicular to the AlN/CrN interfaces. The value of the Young's modulus is very difficult (if not impossible) to comprehend using solely experimental data because models developed for multilayers (see e.g. recent [23]) require the knowledge of the properties of both individual phases AlN and CrN. Some of these input parameters (e.g. the elastic properties) are not available in case of B1-AlN because it does not exist in a bulk form and, consequently, measurements cannot be performed. Although the missing parameters can be conveniently obtained by first principles calculations (e.g., [24]), another issue is that in these very fine superlattices, the volume ratio of bulk and interface regions is very high, and the available continuum mechanics models neglecting the impact of interfaces need to be critically tested. Therefore, in this study, we employ quantum-mechanical calculations (i) to simulate the elastic response of AlN/CrN superlattices and (ii) to evaluate the

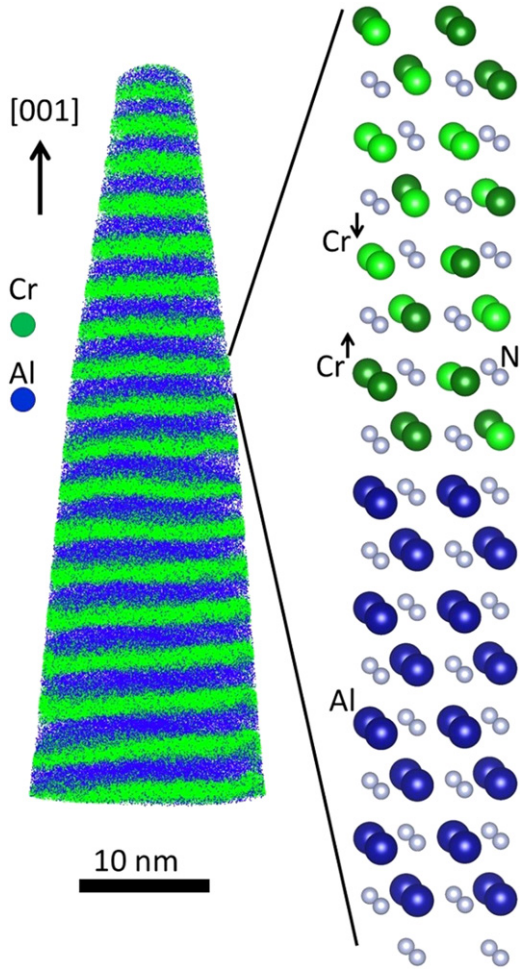

Figure 3. Spatial distribution of Cr and Al in an AlN/CrN superlattice measured by atom probe tomography (left, see also [25]) and the computational model derived from these data (right).

influence of the CrN/AlN interfaces which are typically neglected in classical elastic models but naturally represent part of our first-principles calculations.

Methods

AlN/CrN superlattices were synthesized by radio-frequency (RF) magnetron sputtering, whereas the structural characterization of the microstructure was performed by transmission electron microscopy (TEM) using a JEOL (2200-FS) microscope operated at 200 kV. The chemistry of the superlattice was investigated by atom probe tomography (APT) using a LEAP^{TM} 3000X-HR system. Details on the experiments are given in [25]. The hardness and reduced elastic modulus of the superlattice were determined by nanoindentation at constant load of 6 μN using a Hysitron Triboindenter with a Berkovich tip. The indentation depths were $\leqslant$100 nm, i.e. within 10% of the coating thickness, thus avoiding the influence of the substrate. The Young's modulus of the superlattice was calculated using the elastic modulus (1140 GPa) and Poisson's ratio (0.07) of the indenter in conjunction with the Poisson's ratio of the superlattice, which was estimated as 0.2 [26].

The quantum mechanical calculations within the framework of density functional theory [27, 28] were performed using the Vienna *Ab initio* Simulation Package [29, 30]. The exchange and correlation effects were treated using the generalized gradient approximation as parametrized by Perdew *et al* [31] and implemented in projector augmented wave pseudopotentials [32, 33]. We used a plane-wave cutoff of 450 eV with a $4 \times 4 \times 1$ Monkhorst-Pack k-point mesh for the 128-atomic supercells, yielding a total-energy accuracy in the order of meV. The 128-atomic supercell (see figure 3) serves as our model for an AlN/CrN superlattice. It consists of two parts representing the B1-AlN and B1-CrN phases. The first one is formed by eight ($\sqrt{2} \times \sqrt{2} \times 4$) cubic B1 conventional cells of AlN (see lower part of the computational cell with Al atoms visualized as larger blue spheres

in figure 3). The second region consists of eight ($\sqrt{2} \times \sqrt{2} \times 4$) cubic conventional cells of B1-CrN (see the upper part of the computational cell with Cr atoms visualized as green spheres in figure 3).

The special quasi-random structure (SQS) concept [34] was applied to treat the anti-collinear local magnetic moments of the Cr atoms (see both spin orientations visualized by dark and light green colors, respectively, in figure 3) in order to model an experimentally-found paramagnetic state of CrN [35]. The reliability of our approach is based on previous extensive work focused on CrN by Alling, Abrikosov and their co-workers (see, e.g., [36–40]), specifically their positive comparison of the SQS concept and both the disordered local moments method within the coherent potential approximation and the magnetic sampling method in case of fixed B1 lattices of CrN [37]. Additionally, local atomic relaxations combined with the SQS approach have been shown by Zhou *et al* [24] to have only very limited impact when describing the bulk B1-CrN and the actual distribution of the local anti-parallel magnetic moments within different SQS supercells has been demonstrated to have only very minor impact on the computed properties (see, for example, table 1 in [35]).

The applied periodic boundary conditions produce the superlattice geometry with a bi-layer period about 3.2 nm. Elastic constants were computed by the stress–strain method [24]. Additional tests revealed that, e.g. in case of AlN, the relative changes in elastic constants are about 2% when increasing the plane-wave cutoff energy from 450 to 700 eV (used in [24]). All atomic positions as well as the shape of the supercell were allowed to change so as to minimize the total energy (a full structural optimization). The computed single-crystal elastic constants, as predicted here by *ab initio* calculations for the AlN/CrN superlattice, do not assume tetragonal symmetry as expected for the lamellar geometry when two cubic-symmetry phases are stacked one on top of another along [001]. The reason is that the SQS of the local magnetic moments of the Cr atoms (as our model for the paramagnetic state) in the CrN part of the supercell violates such symmetry. Moakher and Norris [41] provided a rigorous mathematical theory on how to project a tensor of elastic constants with an arbitrary symmetry onto a tensor with a desired crystallographic symmetry (here tetragonal). We use this method in our study as described below. Similar concepts are often used in case of systems with any form of disorder (see e.g. [42–45]).

Results and discussion

The microstructure of the deposited AlN/CrN superlattice was characterized by TEM. Figure 2(a) presents a scanning TEM (STEM) image of the multilayers recorded in high angle annular dark field (HAADF) mode. The image shows chemically very well defined layers as indicated by the chemical contrast provided by the atomic number Z. Additionally, high-resolution (HR) TEM investigations revealed coherency between the multilayers (see figure 2(b)), which is fundamental for comparison with the modeled AlN/CrN superlattice. Nanoindentation experiments performed along the direction perpendicular to the (001) AlN/CrN interfaces yield a Young's modulus of 408 $\pm$ 32 GPa.

In this paper we quantitatively analyze the measured Young's modulus of the as-deposited AlN/CrN superlattice. We use quantum-mechanical calculations to (i) determine elastic constants C_{ij} of the AlN/CrN superlattice and (ii) evaluate the directional dependence of the Young's modulus (using the earlier obtained values C_{ij}) including specifically the [001] direction for which the nano-indentation measurements were performed. The resulting set of elastic constants computed for the AlN/CrN superlattice (essentially a tetragonal system with a lamellar geometry oriented along the [001] direction) is $C_{11} = 456$ GPa, $C_{12} = 145$ GPa, $C_{13} = 146$ GPa, $C_{33} = 500$ GPa, $C_{44} = 155$ GPa and $C_{66} = 214$ GPa. A directional dependence of the corresponding Young's modulus based on this tensor of elastic constants is shown in figure 4 (computed and visualized by the SC-EMA [46–48] library freely accessible at scema.mpie.de).

The predicted value of the Young's modulus along [001] is 428 GPa and falls within the experimental uncertainty of 408 $\pm$ 32 GPa measured by nano-indentation. Additionally, in order to probe any size-dependence of our results with respect to the bi-layer thickness, we performed calculations for twice thinned layers ($\sqrt{2} \times \sqrt{2} \times 2$ cubic B1 conventional cells of both CrN and AlN) and these resulted in elastic constants that only marginally changed, $C_{11} = 480$ GPa, $C_{12} = 142$ GPa, $C_{13} = 138$ GPa, $C_{33} = 481$ GPa, $C_{44} = 150$ GPa and $C_{66} = 207$ GPa. This example neatly shows that quantum-mechanical calculations can be used not only to explain measured data related to nano-scaled superlattices, but also for a reliable prediction of properties of these systems within a theory-guided materials design concept.

When aiming at a high-throughput version of state-of-the-art theory-guided designing concepts, all-atom *ab initio* calculations of the whole two-component superlattice using supercells similar to that depicted in figure 3 are, however, still computationally too intensive (weeks/months of CPU time using multi-processor supercomputers). Therefore, in order to significantly reduce computational costs and enable high-throughput simulations, we assess the performance of a suitable linear-elasticity continuum model of Grimsditch and Nizzoli [49] that is based on the elasticity tensor, the molar ratio, and the crystallographic orientation of each

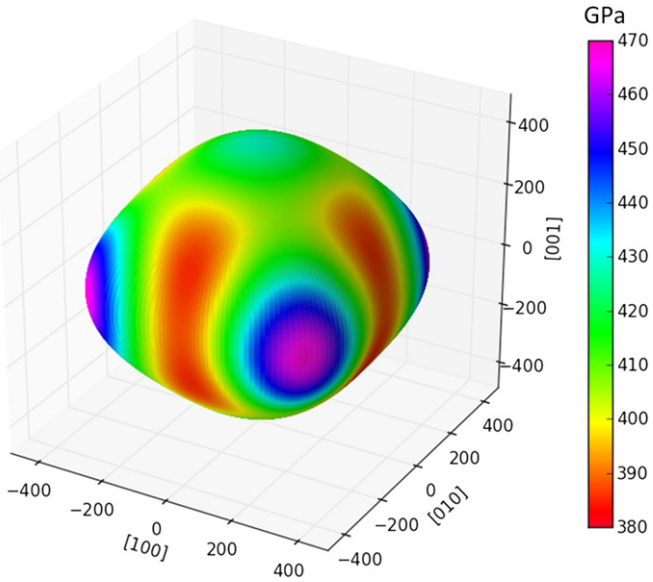

Figure 4. The directional dependence of the Young's modulus (in GPa) of the simulated AlN/CrN superlattice based on *ab initio* calculated elastic constants (computed and visualized by the SC-EMA [46–48] library freely accessible at scema.mpie.de).

individual phase, but disregards any heterogeneity introduced by the layer interface as well as the exact bi-layer spacings. Experimental values of the elasticity tensor have been difficult to obtain for CrN but do exist [50].

The situation is fundamentally different in the case of AlN that crystallizes under normal conditions in a hexagonal B4 phase, and, thus, does not exist as bulk material in the B1 phase that is observed in the AlN/CrN bi-layer structure. Consequently, there are no experimental single-crystal elastic constants of B1-AlN available in literature. Therefore, we propose to use quantum-mechanical calculations to determine the missing elastic parameters of B1-AlN. In order to be on equal footing (and not mix experimental and theoretical values) we use here elastic constants calculated from first principles [24] for both B1-CrN ($C_{11} = 516$ GPa, $C_{12} = 115$ GPa, $C_{44} = 116$ GPa) and B1-AlN ($C_{11} = 426$ GPa, $C_{12} = 167$ GPa, $C_{44} = 306$ GPa) using similar parameters as in the present study, hence providing relevant and comparable predictions. Figure 5 (left) shows that the elasticity of these two phases is qualitatively opposite: B1-AlN (top) is elastically hard along the $\langle 111 \rangle$ and soft along the $\langle 001 \rangle$ directions, while B1-CrN (bottom) is exactly opposite.

Using the above listed *ab initio* predicted single-crystal elastic constants of B1-AlN and B1-CrN as input for the linear-elasticity continuum model of Grimsditch and Nizzoli [49], single-crystal elastic constants of the AlN/CrN superlattice can be predicted. The corresponding directional dependence of the Young's modulus is shown in figure 5 (right-hand part). The superlattice system has a tetragonal symmetry as a consequence of the orientation of the material layers within the superlattice. The Young's modulus along [001] is predicted as 400 GPa, i.e. very close to the measured value of 408 GPa and within the 32 GPa error-bar of the nanoindentation measurements.

The small differences (± 10 GPa) between the directional dependences of the Young moduli of the AlN/CrN superlattice directly predicted from quantum-mechanical simulations (figure 4) and the linear-elasticity continuum model (figure 5 right, color-coded scales are identical in these two cases) are attributed to the following effects. First, the linear-elasticity method of Grimsditch and Nizzoli [49] does not take into account the actual interface (only compatibility and equilibrium of normal stress apply). Second, the linear elastic continuum model is length-scale independent, i.e. it does not consider the thickness of the layers but only their volume fraction, and hence would predict the same result for any kind of planar dispersion of the AlN/CrN layers. Third, when we used the method of Grimsditch and Nizzoli, the input single-crystalline elastic constants were those computed for equilibrium lattice parameters of each of the two phases (4.07 Å for B1-AlN and 4.15 Å for B1-CrN) whereas the all-atom simulated AlN/CrN superlattice is coherent and has an in-plane lattice parameter of 4.11 Å that is common to both phases (and different from their equilibrium lattice parameters) and corresponds to the minimum energy of the whole superlattice system. Our approach here reflects the fact that, without either quantum-mechanical calculations or advanced experimental measurements the equilibrium lattice parameter of the AlN/CrN superlattice, this value would not be known. This is even more true in case of elastic constants of individual phases B1-AlN and B1-CrN (with these two materials artificially kept off their own individual equilibria at the equilibrium lattice parameter of the AlN/CrN superlattice). This fact can be crucial

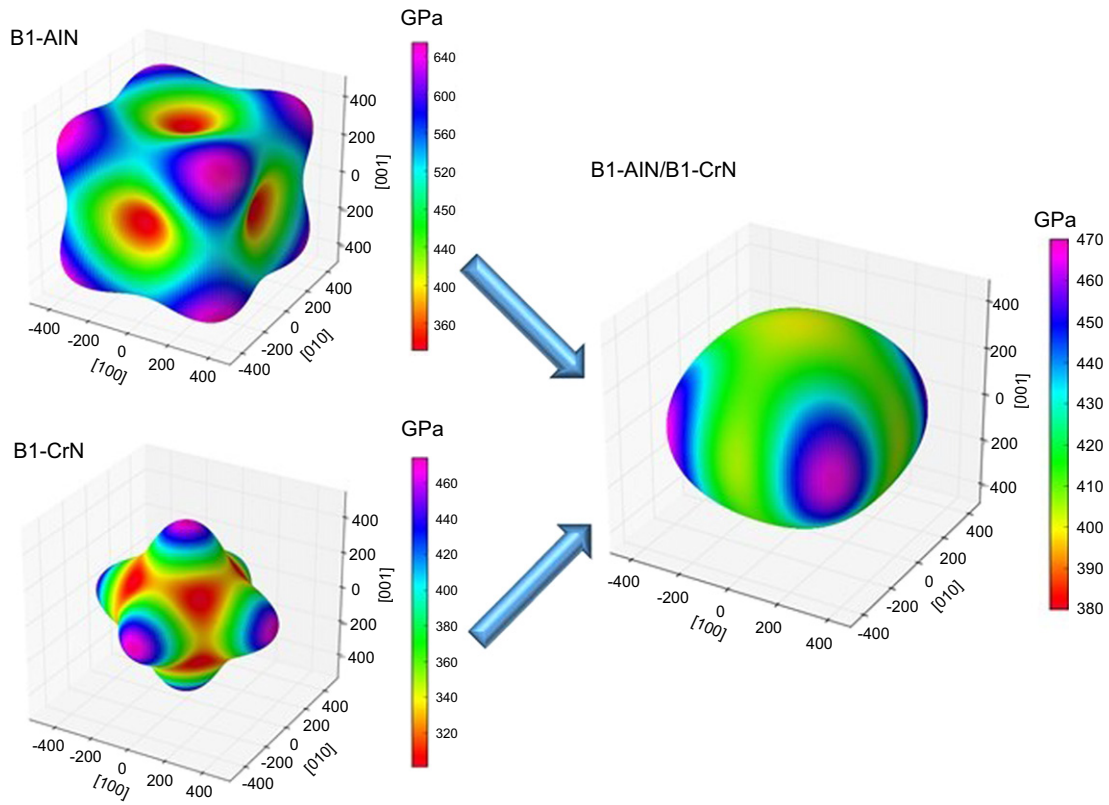

Figure 5. Directional dependences of the Young moduli of B1-AlN (top left), B1-CrN (bottom left) and the AlN/CrN multilayer (right) computed by a linear-elasticity approach (schematically visualized by the arrows) of Grimsditch and Nizzoli [49] using *ab initio* determined single-crystal elastic constants of B1-AlN and B1-CrN as published in [24] as input. Please mind different color-coded scales.

when applying the approach of Grimsditch and Nizzoli to other materials systems with more mismatching lattice parameters (bench marking quantum-mechanical calculations would be necessary in these cases).

Considering the close match between all three values of the Young modulus established for the layer normal direction [001] by two theoretical (400 and 428 GPa) and one experimental method (408 $\pm$ 32 GPa), the comparably crude linear-elasticity approach [49] appears to be a suitable candidate for high-throughput screening of elastic properties. A particular speed advantage is the applicability of the same (equilibrium bulk) elasticity tensors for different crystallographic orientations of layer interfaces, e.g. {111} or {110} instead of {100} used here. In contrast, atomic and electronic structure quantum-mechanical calculations would have to be re-run with different supercells specifically constructed for each interface orientation (consuming months to years of CPU time). Hence, the approach of Grimsditch and Nizzoli allows to explore a vast space of different crystallographic orientations of the interface separating the two deposited phases probing the opposite hard/soft crystallography of the two deposited phases (see subfigures on the left of figure 5).

In order to examine elastic properties of CrN/AlN superlattices with different interface orientations, we limit ourselves to situations when both phases have the same molar fraction and are deposited with the same crystallographic orientation repetitively one on top of the other. Employing the approach of Grimsditch and Nizzoli for different interface orientations and molar fraction of B1-AlN phase, we have computed the Young's modulus that would be detected in the direction perpendicular to these interfaces. A directional dependence of the Young's modulus as a function of molar fraction of B1-AlN is shown in figure 6 for each of the three main crystallographic interface orientations, (001), (110) and (111). As seen, a much higher Young's modulus (even over 600 GPa) in the direction perpendicular to the interface can be achieved if the phases are deposited on top of each other along the $\langle 111 \rangle$ crystallographic direction.

Most importantly, this rather superior stiffness is not due to the stiffness of CrN, i.e., the phase that exists as a bulk under ambient conditions, but mostly due to the B1-AlN (see the directional dependences of both phases on the left of figure 5), that is not stable in the B1 crystal structure as a bulk and is stabilized in the form of nano-sized layers inside of the studied superlattice. The theory-guided materials design thus enters potentially unlimited area of metastable material phases, which do not exist as a bulk, but that can provide unprecedented/superior properties to nano-patterned composites in which they would be stabilized in crystal structures determined by other composite components. As there are no experimental data for these metastable phases,

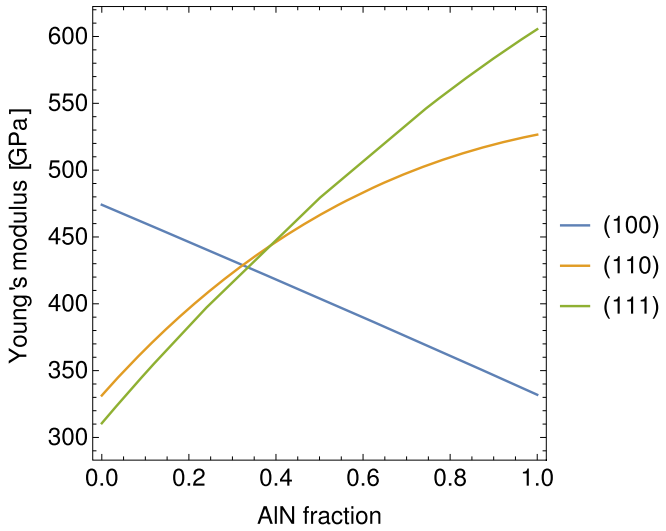

Figure 6. Computed directional dependence of the Young's modulus (GPa) of the superlattice predicted by the approach of Grimsditch and Nizzoli [49], that would be detected in the direction perpendicular to the interfaces between both phases, as a function of crystallographic orientation of these interfaces, i.e. the crystallographic direction along which both phases are repetitively deposited one on top of the other (visualized as a function of the molar fraction of the B1-AlN phase).

which normally do not exist as a bulk, quantum-mechanical calculations can serve as an excellent guide in this uncharted territory. We thus pave a path towards a theory-guided fine-tuning of the overall superlattice Young modulus responding to application-driven industrial needs by changing either/both properties of (meta-)stable phases present in the superlattice and/or interface orientations.

Conclusions

We have employed quantum-mechanical calculations to predict elastic properties of AlN/CrN superlattices and compared our results to nanoindentation data collected from coherent multilayers deposited by reactive RF magnetron sputtering. The *ab initio* predicted Young modulus (428 GPa) along [001] is in excellent agreement with the measured nano-indentation value (408 $\pm$ 32 GPa). Aiming at a future high-throughput materials design of superlattices, we assessed predictions from a linear-elasticity continuum model [49]. Required elastic constants of B1-CrN and B1-AlN phases were calculated *ab initio* and their volume fractions determined by APT and HRTEM. Since excellent agreement between predictions and experiment is reached also in this case—at much reduced computational cost—we speculate that Grimsditch and Nizzoli's approach [49] is suitable for designing nano-scaled superlattices by varying the crystallographic orientation of the layer interface.

The role of quantum-mechanical calculations is irreplaceable here for two reasons. First, in the studied superlattice, AlN occurs as metastable B1 (NaCl) phase for which experimental values do not exist. Therefore, *ab initio* calculations of individual bulk phases are the only way to obtain the unknown parameters. Second, the success of the linear-elasticity approach might be specific to the studied B1-AlN/CrN superlattice (with small mismatch in lattice parameter) and bench marking quantum-mechanical calculations should be performed before applying the continuum approximation in a high-throughput manner to superlattices containing other phases. The combined approach nevertheless allows to explore a vast and yet uncharted territory of different orientations of multilayers and individual phases that, depending on their properties, can be very rich and potentially providing unprecedented/superior properties. A path towards a high-throughput theory-guided optimization of Young modulus in nano-scale bi-layer composites by changing the properties of (meta-)stable constituents and/or layer interface orientations [51–53] is thus paved for future exploration.

Acknowledgments

We would like to thank to Dr Maxim N Popov from the Materials Center Leoben Forschung GmbH (MCL), in Leoben, Austria, for his drawing our attention to Grimsditch and Nizzoli's modeling approach. MF acknowledges financial support from the Academy of Sciences of the Czech Republic through the Fellowship of Jan Evangelista Purkyně and access to the computational resources provided by the MetaCentrum under the program LM2010005 and the CERIT-SC under the program Centre CERIT Scientific Cloud, part of the

Operational Program Research and Development for Innovations, Reg. No. CZ.1.05/3.2.00/08.0144. DH acknowledges financial support by the Austrian Science Fund FWF within the START Project Y371. The authors gratefully acknowledge funding of the experimental part by the German Research Foundation (DFG) (Contract CH 943/1-1). The computational supercell in figure 3 was visualized using the VESTA package [54–56].

References

[1] Holleck H J 1986 *J. Vac. Sci. Technol.* A **4** 2661
[2] Zlatanovic M, Kakas D, Mazibrada L, Kunosic A and Münz W D 1994 *Surf. Coat. Technol.* **64** 173
[3] Staia M H, Puchi E S, Lewis D B, Cawley J and Morel D 1996 *Surf. Coat. Technol.* **86–87** 432
[4] Yashar P C and Sproul W D 1999 *Vacuum* **55** 179
[5] Kim D G, Seong T Y and Baik Y J 2002 *Surf. Coat. Technol.* **153** 79
[6] Shinn M, Hultman L and Barnett S A 1992 *J. Mater. Res.* **7** 901
[7] Helmersson U, Todorova S, Barnett S A, Sundgren J E, Markert L S and Greene J E 1987 *J. Appl. Phys.* **62** 481
[8] Yang Q, He C, Zhao L R and Immarigeon J P 2002 *Scr. Mater.* **46** 293
[9] Yang Q and Zhao L R 2003 *J. Vac. Sci. Technol.* A **21** 558
[10] Park J K and Baik Y J 2005 *Surf. Coat. Technol.* **200** 1519
[11] Lin J, Moore J J, Mishra B, Pinkas M, Zhang X and Sproul W D 2009 *Thin Solid Films* **517** 5798
[12] Kim G S, Lee S Y, Hahn J H and Lee S Y 2003 *Surf. Coat. Technol.* **171** 91
[13] Bardi U, Chenakin S P, Ghezzi F, Giolli C, Goruppa A, Lavacchi A, Miorin E, Paruga C and Tolstogouzov A 2005 *Appl. Surf. Sci.* **252** 1339
[14] Tien S K and Duh J G 2006 *Thin Solid Films* **494** 173
[15] Tien S K, Duh J G and Lee J W 2007 *Surf. Coat. Technol.* **201** 5138
[16] Kim B S, Kim G S, Lee S Y and Lee B Y 2008 *Surf. Coat. Technol.* **202** 5526
[17] Paldey S and Deevi S C 2003 *Mater. Sci. Eng.* A **342** 58
[18] Mayrhofer P H, Mitterer C, Hultman L and Clemens H 2006 *Prog. Mater. Sci.* **51** 1032
[19] Mayrhofer P H, Rachbauer R, Holec D, Rovere F and Schneider J M 2014 *Comprehensive Materials Processing* ed S Hashmi, G F Batalha, C J V Tyne and B Yilbas (Oxford: Elsevier) pp 355–88
[20] Paulitsch J, Schenkel M, Zufraß T, Mayrhofer P H and Münz W-D 2010 *Thin Solid Films* **518** 5558
[21] Schlögl M, Mayer B, Paulitsch J and Mayrhofer P H 2013 *Thin Solid Films* **545** 375
[22] Chawla V, Holec D and Mayrhofer P H 2014 *Thin Solid Films* **565** 94–100
[23] Vannucci P 2013 *J. Elast.* **112** 199–215
[24] Zhou L, Holec D and Mayrhofer P H 2013 *J. Appl. Phys.* **113** 043511
[25] Tytko D, Choi P-P and Raabe D 2015 *Acta Mater.* **85** 32
[26] Ichimura H and Ando I 2001 *Surf. Coat. Technol.* **145** 88
[27] Hohenberg P and Kohn W 1964 *Phys. Rev.*B **136** B864
[28] Kohn W and Sham L J 1965 *Phys. Rev.*A **140** A1133
[29] Kresse G and Hafner J 1993 *Phys. Rev.* B **47** 558
[30] Kresse G and Furthmüller J 1996 *Phys. Rev.* B **54** 11169
[31] Perdew J P, Burke K and Ernzerhof M 1996 *Phys. Rev. Lett.* **77** 3865
[32] Blöchl P E 1994 *Phys. Rev.* B **50** 17953
[33] Kresse G and Joubert D 1999 *Phys. Rev.* B **59** 1758
[34] Wei S-H, Ferreira L G, Bernard J E and Zunger A 1990 *Phys. Rev.* B **42** 9622
[35] Zhou L, Körmann F, Holec D, Bartosik M, Grabowski B, Neugebauer J and Mayrhofer P H 2014 *Phys. Rev.* B **90** 184102
[36] Alling B, Marten T and Abrikosov I A 2010 *Nat. Mater.* **9** 283
[37] Alling B, Marten T and Abrikosov I A 2010 *Phys. Rev.* B **82** 184430
[38] Steneteg P, Alling B and Abrikosov I A 2012 *Phys. Rev.* B **85** 144404
[39] Lindmaa A, Lizárraga R, Holmström E, Abrikosov I A and Alling B 2013 *Phys. Rev.* B **88** 054414
[40] Mozafari E, Alling B, Steneteg P and Abrikosov I A 2015 *Phys. Rev.* B **91** 094101
[41] Moakher M and Norris A N 2006 *J. Elast.* **85** 2015
[42] Tasnádi F, Abrikosov I A, Rogström L, Almer J, Johansson M P and Odén M 2010 *Appl. Phys. Lett.* **97** 231902
[43] Tasnádi F, Odén M and Abrikosov I A 2012 *Phys. Rev.* B **85** 144112
[44] von Pezold J, Dick A, Friák M and Neugebauer J 2010 *Phys. Rev.* B **81** 094203
[45] Holec D, Tasnádi F, Wagner P, Friák M, Neugebauer J, Mayrhofer P H and Keckes J 2014 *Phys. Rev.* B **90** 184106
[46] Titrian H, Aydin U, Friák M, Ma D, Raabe D and Neugebauer J 2013 *Mater. Res. Soc. Symp. Proc.* vol 1524
[47] Friák M, Counts W A, Ma D, Sander B, Holec D, Raabe D and Neugebauer J 2012 *Materials* **5** 1853
[48] Zhu L-F *et al J. Mech. Behav. Biomed. Mater.* **20** 2013296
[49] Grimsditch M and Nizzoli F 1986 *Phys. Rev.*B **33** 5891
[50] Cheng Y H, Browne T and Heckerman B 2011 *Wear* **271** 775
[51] Prakash A, Guénolé J, Wang J, Müller J, Spiecker E, Mills M J, Povstugar I, Choi P, Raabe D and Bitzek E 2015 *Acta Mater.* **92** 33
[52] Herbig M, Raabe D, Li Y J, Choi P, Zaefferer S and Goto S 2013 *Phys. Rev. Lett.* **112** 126103
[53] Kuzmina M, Herbig M, Ponge D, Sandlöbes S and Raabe D 2015 *Science* in press
[54] Momma K and Izumi F 2011 *J. Appl. Crystallogr.* **44** 1272
[55] Momma K and Izumi F 2008 *J. Appl. Crystallogr.* **41** 653
[56] Momma K and Izumi F 2006 Commission on crystallographic computing *IUCr Newsletter* No. 7, p 106